

Three Major Failed Rifts in Central North America: Similarities and Differences

Reece Elling¹, Seth Stein¹, Carol A. Stein², Kerri Gefeke²

¹Earth & Planetary Sciences, Northwestern University, Evanston, IL 60208

²Earth & Environmental Sciences, University of Illinois, Chicago, IL 60607

Abstract

The North American craton preserves over a billion years of geologic history, including three major rifts that failed rather than evolving to continental breakup and seafloor spreading. The Midcontinent Rift (MCR) and Southern Oklahoma Aulacogen (SOA) show prominent gravity anomalies due to large volumes of igneous rift-filling rock. The Reelfoot Rift (RR), though obscure in gravity data, is of interest due to its seismicity. The ~1.1 Ga MCR records aspects of the assembly of Rodinia, whereas the ~560 Ma SOA and RR formed during the later breakup of Rodinia and subsequent assembly of Pangea. Comparative study of these rifts using geophysical and geological data shows intriguing similarities and differences. The rifts formed in similar tectonic settings and followed similar evolutionary paths of extension, magmatism, subsidence, and inversion by later compression, leading to similar width and architecture. Differences between rifts reflect the extent to which these processes occurred. Further study of failed rifts would give additional insight into the final stages of continental rifting and early stages of seafloor spreading.

Introduction

Plate tectonics shapes the evolution of the continents and oceans via the Wilson cycle, in which continents rift to form new oceans. In such cases, many rifts evolve to passive continental margins. However, some rifts fail before continental breakup and remain as fossil features within continents, largely buried beneath the surface and studied primarily with gravity and seismic surveys. Failed rifts preserve a snapshot of the rifting process before the beginning of seafloor spreading and thus give insight into late stages of continental rifting and formation of passive continental margins (Stein et al., 2018a; 2021).

North America contains multiple impressive failed rifts (Fig. 1), preserving important aspects of the fabric of over a billion years of geologic history in Laurentia, its Precambrian core (Whitmeyer and Karlstrom, 2007; Marshak and van der Pluijm, 2021). We focus on three major

33 failed rifts, covering ~10% of central North America. One, the Midcontinent Rift (MCR), is a
34 prominent feature in geophysical maps of the region. Due to its size and the availability of
35 geophysical and geological data, the MCR has been the focus of many studies giving insight into
36 its evolution, role in the assembly of Rodinia, and processes of rifting and passive margin
37 evolution. Two other failed rifts, the Southern Oklahoma Aulacogen (SOA) and Reelfoot Rift (RR),
38 have also been subjects of much interest. Parts of the SOA lie within the basement near and
39 below the Anadarko Basin, a major oil and gas producing basin. Thus, some of its features are
40 well studied, but the overall structure is rarely the primary target of study. The RR and its northern
41 extensions, on the other hand, have little interest for the energy industry but are of interest due to
42 their active seismicity.

43 These three failed rifts are grossly similar, with similar tectonic origins and structural
44 features, but with interesting differences highlighting aspects of their evolution. These are shown
45 by gravity data that are uniformly sampled across the central U.S. (Fig. 1). In contrast, other data
46 available differ from area to area. In particular, high-quality seismic reflection data giving detailed
47 structure at depth that allows modeling of the rift's evolution are available only across the part of
48 the MCR below Lake Superior. Conversely, EarthScope local array data showing structure
49 beneath the rift are available only across parts of the MCR's west arm and Reelfoot Rift.

50 Using gravity data from the PACES (Keller et al., 2006) and TOPEX datasets (Sandwell
51 et al., 2013), we extracted profiles 150 km long and ~50 km apart across each rift (Fig. 1B). Fig.
52 1C shows each rift's mean Bouguer anomaly and standard deviation. The mean profiles show
53 differences between rifts, reflecting their tectonic origin and subsurface structure. The MCR's west
54 arm shows large gravity highs (~80 mGal) bounded by ~20 mGal lows on either side of the rift
55 basin. In contrast, the MCR's east arm has a positive anomaly half that of the west arm and lacks
56 bounding lows. The Southern Oklahoma Aulacogen has a ~60 mGal positive anomaly, similar to
57 the MCR, whereas the Reelfoot Rift shows only a minor (~10-15 mGal) positive anomaly despite
58 forming about the same time as the SOA.

59 The profiles are generally similar in width and form, but differ in amplitude, suggesting
60 general similarities between the rifts. We use the mean gravity profiles augmented with seismic
61 and other data, combined with results from earlier studies, to model the rifts' general subsurface
62 structures. We start with the hypothesis that the rifts are similar, and so when needed use
63 inferences from one rift to gain insight into others, to the extent that the data permit. Although the
64 models reflect limitations of the available data, they characterize average structure along the rifts
65 and illustrate similarities and differences between them. The similarities and differences reflect

66 the combined effects of a sequence of rifting, volcanism, sedimentation, subsidence,
67 compression, erosion, and later effects (Stein et al., 2015; Elling et al., 2020). They give insight
68 into how rifts evolve and are useful when studying other failed or active rifts elsewhere.

69

70 **Midcontinent Rift**

71 The Midcontinent Rift (MCR), a 3000 km long band of more than 2 million km³ of buried
72 igneous and sedimentary rocks that outcrop near Lake Superior, has been extensively studied,
73 as reviewed by Ojakangas et al. (2001) and Stein et al. (2018a). To the south, it is buried by
74 younger sediments, but easily traced because the rift-filling volcanic rocks are dense and highly
75 magnetized. The western arm extends southward to Oklahoma, as shown by positive gravity
76 anomalies and similar-age diffuse volcanism (Bright et al., 2014). The eastern arm extends
77 southward to Alabama (Keller et al., 1983; Stein et al., 2014, 2018ab; Elling et al., 2020). The
78 MCR likely formed as part of rifting of the Amazonia craton (now in northeastern South America)
79 from Laurentia, the Precambrian core of North America at 1.1 Ga, between collisional phases of
80 the Grenville Orogeny (Stein et al., 2014, 2018ab). Surface exposures, seismic data, and gravity
81 data delineate rift basins filled by thick basalt layers and sediments, underlain by thinned crust
82 and an underplate unit, presumably the dense residuum from the magma extraction (Vervoort et
83 al., 2007; Stein et al., 2018a). The rift was later massively inverted by regional compression,
84 uplifting the volcanic rocks so that some are exposed at the surface today. The MCR has little
85 seismicity along most of its length, but portions in Kansas and Oklahoma experienced seismicity
86 and Phanerozoic deformation (Burberry et al., 2015; Levandowski et al., 2017).

87 We developed models for each arm (Figs. 2AB), because the west arm's larger gravity
88 anomaly indicates differences in magma volume and tectonic evolution. For simplicity, the models
89 use average densities of the sediment, igneous rift fill, underlying crust, underplate, and mantle.
90 We began with GLIMPCE seismic reflection profiles across Lake Superior that give the best
91 available image of structure at depth in the MCR (Green et al., 1989) and permit detailed modeling
92 of its evolution (Stein et al., 2015). We also considered prior gravity models across parts of the
93 MCR (Mayhew et al., 1982; Shay and Trehu, 1993). EarthScope data (Zhang et al., 2016)
94 provided values for the depth and thickness of the volcanics and underplate along the west arm
95 and showed that structure below the west arm resembles that below Lake Superior, suggesting
96 that the structure along the entire MCR is similar. On either side of the central rift basin, basins

97 ~5 km thick resulting from post-rift sedimentation produce bounding gravity lows. The sediments
98 are much thinner over the central basin as a result of inversion, uplift, and erosion after rift failure.

99 We model the east arm as similar to the west. Because the east arm does not show
100 bounding gravity lows, the model does not include bounding basins. We include an underplate
101 like that below the west arm, although seismic data needed to resolve it are lacking, because
102 such underplates are also seen below the Reelfoot Rift, have been proposed below the SOA, are
103 common in rifts worldwide (Thybo and Artemieva, 2013; Rooney et al., 2017) and are expected
104 given the igneous rift fill (Vervoort et al., 2007). The largest difference between the models is the
105 thickness of rift-filling volcanics; the west arm contains 20–25 km of volcanics, whereas the east
106 arm contains 10–15 km. The dense igneous rocks affect the gravity anomaly much more than the
107 underplate, so the geometry of the volcanics in the east arm was adjusted to match the gravity
108 profiles.

109

110 **Southern Oklahoma Aulacogen**

111 The Southern Oklahoma Aulacogen (Walper, 1977) is a linear alignment of extensively
112 inverted rift structures perpendicular to the southern tip of the MCR's west arm. Its main structures
113 are the Wichita uplift (and associated igneous provinces) and Anadarko basin. Both the SOA and
114 RR (discussed shortly) initiated as the Cuyania block, also known as the Argentine Precordillera,
115 rifted away from Laurentia (Thomas, 2011; Whitmeyer and Karlstrom, 2007). Rifting is thought to
116 have begun in Latest Precambrian, but the oldest dates come from SOA igneous rocks dated at
117 ~540 Ma (Wall et al., 2020).

118 The SOA's geologic and tectonic history has three major phases. The first involved
119 emplacement of the Wichita Igneous Province during development of a rift beginning in Late
120 Proterozoic to Mid-Cambrian (Brewer et al., 1983; Perry, 1989). Extensional and transtensional
121 tectonism within the SOA developed during the Latest Precambrian/Cambrian opening of the
122 southern Iapetus Ocean as part of Rodinia's breakup. Following rift failure, thermal subsidence
123 allowed deposition of thick sedimentary sequences, marking the onset of the Anadarko Basin
124 formation (Perry, 1989; Johnson, 2008). Finally, Late Mississippian through Pennsylvanian
125 compression inverted the SOA and formed a NE-trending fold-thrust belt containing the Wichita
126 and Arbuckle Mountains. The compression is believed to be related to North America's collision
127 with Africa and South America during the Alleghenian Orogeny (Kluth and Coney, 1981) or
128 tectonic activity along North America's western and southwestern margins (Lawton et al., 2017;

129 Leary et al., 2017). The SOA exposes only a fraction of its extent in the Wichita Mountains, and
130 contains more than 210,000 km³ of buried mafic rocks up to 10 km thick along the entire rift
131 (Hanson et al., 2013), along with a large volume of felsic igneous rocks in interbedded rhyolites
132 and granites. Emplacement and subsequent inversion of the igneous rocks yielded a positive
133 gravity anomaly of ~60 mGal, similar to the average of the MCR arms.

134 Our SOA model is modified from Keller and Stephenson's (2007) model based on gravity,
135 seismic, aeromagnetic, surface mapping, and drilling data. Seismic reflection data were used to
136 constrain the location and thicknesses of the gabbroic and felsic intrusions producing the large
137 positive anomaly. We simplified their model for comparison with the other rifts. Sedimentary basin
138 rocks were averaged into a few units, and bodies within the gabbroic intrusion that increased in
139 density with depth in the original model were averaged to a single density. Keller and Baldrige
140 (1995) proposed the presence of an underplate, which is consistent with the gravity data and
141 included in our model, though seismic data adequate to confirm (or disprove) its presence are not
142 available.

143

144 **Reelfoot Rift**

145 The Reelfoot Rift underlies the Upper Mississippi Embayment, a broad trough with a
146 complex history of rifting and subsidence (Catchings, 1999). The NE-trending graben of the RR
147 is 70 km wide and more than 300 km long. Reflection profiles suggest mafic alkalic plutons from
148 several episodes of faulting and intrusive activity (Mooney et al., 1983). The RR is believed to
149 have experienced multiple phases of subsidence (Ervin and McGinnis, 1975), with the earliest
150 rifting in the Latest Precambrian associated with wide-spread rifting along North America's
151 margins during the breakup of Rodinia. The rift basin primarily developed during this Cambrian-
152 Ordovician event. Later subsidence, perhaps as late as the Cretaceous, is associated with
153 emplacement of mafic igneous intrusives inside the rift and deposition of several kilometers of
154 sediments that bury them (Hildenbrand and Hendricks, 1995; Cox and Van Arsdale, 2002).
155 Relative to the MCR and SOA, the RR experienced significantly less volcanic activity during rifting,
156 and its subsidence influenced the sedimentation and drainage of major rivers such as the
157 Mississippi. The sedimentation has been proposed to have triggered the present seismicity (New
158 Madrid seismic zone) on faults remaining from the rifting (Calais et al., 2010).

159 We developed our model by modifying one by Liu et al. (2017) based on their work and
160 earlier models constrained by seismic refraction, gravity, and magnetic data (Mooney et al., 1983;

161 Braile et al., 1986; Nelson and Zhang, 1991). Earlier studies identified an underplate, or "rift
162 pillow", whose location is constrained by Liu et al.'s (2017) results. An underplate has also been
163 observed along the RR's northeastern extension (Aziz Zanjani et al., 2019). Our model replicates
164 the lack of a large gravity anomaly, in contrast to the other rifts. An implication of the model is that
165 the RR contains far less high-density volcanics than the other rifts, perhaps because it extended
166 less. Low-density Quaternary sediments of the Mississippi River basin overlying the rift rocks also
167 contribute to the minimal anomaly.

168

169 **Similarities and Differences**

170 Comparing the three rifts' average gravity profiles and subsurface structures inferred in
171 part from them illustrates similarities and differences between the rifts.

172 **Tectonic setting:** All three formed during rifting associated with Laurentia's interactions
173 within the supercontinent of Rodinia. The MCR formed between compressional phases of the
174 Grenville Orogeny that assembled Rodinia (e.g., Hynes and Rivers, 2010). Its formation was likely
175 associated with rifting between Laurentia and Amazonia during a plate boundary reorganization
176 (Stein et al., 2014, 2018b) (Fig. 3A), although details of Amazonia's location and motion are not
177 well constrained at this time because of limited paleomagnetic data (Tohver et al., 2006; Li et al.,
178 2008).

179 Additional evidence for this view comes from a change in Laurentia's absolute plate motion
180 at this time (Scotese and Elling, 2017). Its apparent polar wander (APW) path shows a major
181 cusp, commonly referred to as the Logan Loop (Swanson-Hysell et al., 2019), recorded by the
182 MCR's volcanic rocks (Fig. 3C). Cusps in APW paths have been observed elsewhere when
183 continents rift apart (Gordon et al., 1984). A similar cusp appears ~600 Ma (Fig. 3C), during
184 opening of the Iapetus Ocean, as the Argentine Precordillera microcontinent rifted from the
185 Wichita embayment on Laurentia's SE margin (Whitmeyer and Karlstrom, 2007; Thomas, 2011).
186 Both the SOA and RR opened as arms of this triple junction but ultimately failed.

187

188 **Spatial scale and architecture:** The three rifts have similar spatial scales and structures
189 that seem to characterize failed rifts. Their central grabens, filled with volcanic and sedimentary
190 rocks, are bounded by faults that presumably had normal fault motion during extension. Despite
191 structural differences discussed below, all three rifts are ~60-80 km wide, suggesting that failed

192 rifts are consistent with observations that presently spreading rifts had initial widths controlled by
193 crustal structure rather than the extension history (Allemand and Brun, 1991)

194 For the MCR and SOA, the rifting faults were reactivated as reverse faults during
195 subsequent inversion. The SOA's gravity high reflects structural inversion of basaltic and
196 gabbroic material in the Wichita Mountains, but significant amounts of rift-fill remain buried
197 beneath the Anadarko Basin (Keller and Stephenson, 2007). Although the RR looks similar
198 overall, it was not significantly reactivated by later inversion. This left its rift-filling volcanics deeper
199 in the subsurface, causing the absence of a positive gravity anomaly. This effect is illustrated by
200 a model showing the gravity anomaly at different stages in the MCR's evolution (Fig. 4), derived
201 from cross-section-balanced reconstructions from GLIMPCE data. In early rifting stages, dense
202 volcanics near the surface would have caused a large positive anomaly. Subsequent deposition
203 of low-density sediments and subsidence that depressed the volcanics would have caused a
204 gravity low. Eventually, inversion of the rift and erosion and removal of low-density sediments
205 brought the volcanics closer to the surface, causing today's gravity high. Without this inversion, a
206 positive anomaly would not have developed.

207 We explored the hypothesis that inversion is crucial for producing a positive gravity
208 anomaly using the SOA and RR. The SOA experienced up to 15 km of inversion in the late
209 Paleozoic (Keller and Stephenson, 2007). "Uninverting" the rift by re-burying the gabbroic fill 12
210 km below a sedimentary basin eliminates the positive anomaly (Fig 4E). Hence the SOA's gravity
211 high largely reflects the inversion. Conversely, because the RR did not experience significant
212 inversion, its rift basin is buried beneath low density sediments. Inverting the RR by 3 km and
213 removing sediments overlying the basin (Fig. 4F) produces a positive anomaly due to the high-
214 density igneous rift fill being much nearer to the surface.

215 **Igneous rock volumes:** There are interesting differences in the volumes of rift volcanics.
216 The MCR is ~ 3000 km long and contains over 2 million km³ of buried igneous rocks, while the
217 SOA and RR are both roughly 1/10 the length of the MCR and contain significantly less volcanics.
218 Although the SOA's volcanic package produces a large positive gravity anomaly, it contains only
219 about 1/10 as much volcanics as the MCR (Hanson et al., 2013).

220 The differences appear in the cross sections. Volcanics in MCR's west and east arms
221 have average cross-sectional areas of 1100 km² and 680 km², the SOA has an average cross-
222 sectional area of 470 km², whereas the RR's cross-sectional area is much smaller (160 km²).
223 How these differences arose is unclear. The volumes of igneous rocks produced in rifting can

224 reflect two effects. The first is passive rifting in which extension due to far-field forces causes
225 lithospheric thinning and inflow of hot asthenosphere, such that greater extension produces more
226 melt (Koptev et al., 2015). The second involves an upwelling thermal plume, such that melt is
227 generated by elevated mantle temperatures beneath the lithosphere (Burov and Gerya, 2014).
228 The relative roles of these and other possible rifting processes (King, 2007) are extensively
229 debated but remain unclear (Foulger, 2010). Both active and passive rifting have been invoked to
230 explain the volumes of volcanic rocks at rifted continental margins (White and McKenzie, 1989;
231 Richards et al., 1989; van Wijk et al., 2001). Gallahue et al. (2020) find evidence for both
232 processes on continental margins, with passive rifting having a stronger effect.

233 A plume contribution has been inferred for the MCR from petrologic and geochemical data
234 (Nicholson et al., 1997; White, 1997; Davis et al., 2021), consistent with the enormous volume of
235 volcanic rocks making it a Large Igneous Province (Stein et al., 2015). The large volume of MCR
236 rocks also likely reflects Precambrian mantle temperatures higher than today's (Korenaga, 2013).
237 The difference between west and east arms likely reflects a difference in the amount of extension
238 during rifting (Merino et al., 2013; Elling et al., 2020). The smaller cross-sectional areas of
239 volcanics in the SOA and RR probably do not require assuming a plume. The simplest explanation
240 of the differences between these two rifts, which formed about the same time in similar events, is
241 that the RR had less extension and inversion.

242 Our models include underplates beneath the rifts because seismic data from the MCR's
243 west arm and RR show them, and underplates are typically observed at presently spreading rifts.
244 Because underplates are thought to form from residual melt after extraction of low-density lavas,
245 we expect their size to be proportional to the volume (cross-sectional area) of volcanics, as
246 observed for rifted continental margins (Gallahue et al., 2020). Hence the similar underplates
247 beneath the western MCR and RR are surprising, given that the MCR has roughly ten times more
248 volcanics in cross section. One possible explanation is that in addition to the volcanics in our RR
249 model, another volcanic unit, a mafic high-density upper crustal layer also exists. Liu et al. (2017)
250 suggest this possibility while noting that such a layer is not required by the data and would be
251 "rare, if not previously unrecognized, for continental rifts." Another possibility is that during mid-
252 Cretaceous, as the area passed over the Bermuda plume (Cox and Van Arsdale, 2002), plume-
253 derived material may have been augmented the underplate. Improved understanding of the
254 relation between the volcanics and underplate would be helpful in understanding the transition
255 between the final stages of continental rifting and early stages of seafloor spreading.

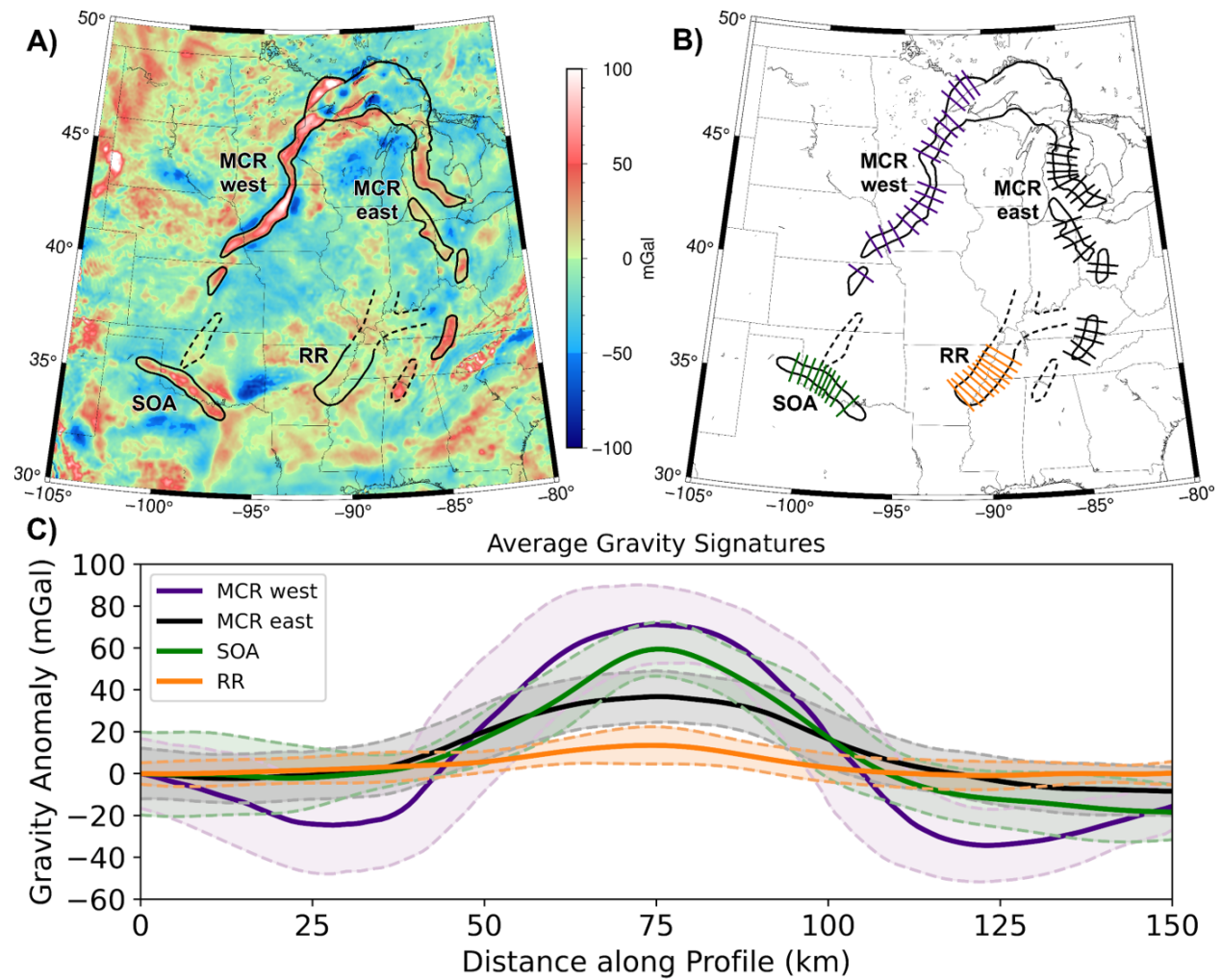
256 **References**

- 257 Allemand, P., Brun, J. 1991, Width of continental rifts and rheological layering of the lithosphere:
258 Tectonophys., v.188, p.63-69
- 259 Aziz Zanjani, A., Zhu, L., Herrmann, R., Liu, Y., Gu, Z., Conder, J., 2019, Crustal structure beneath
260 the Wabash Valley Seismic Zone from joint inversion of receiver functions and surface-
261 wave dispersion: J. Geophys. Res., v.124, p.7028-7039
- 262 Braile, L., Hinze, W., Keller, G., Lidiak, E., Sexton, J., 1986, Tectonic development of the New
263 Madrid rift complex: Tectonophys., v.131, p.1-21
- 264 Brewer, J., Good, R., Oliver, J., Brown, L., Kaufman, S., 1983, COCORP profiling across the
265 Southern Oklahoma aulacogen: Geology, v.11, p.109-114
- 266 Bright, R., Amato, J., Denyszyn, S., Ernst, R., 2014, U-Pb geochronology of 1.1 Ga diabase in
267 the southwestern United States: Lithos., v.6, p.135-156
- 268 Burberry, C., Joeckel, R., Korus, J., 2015, Post-Mississippian tectonics of the Nemaha Tectonic
269 Zone and Mid-Continent Rift System: Mountain Geologist, v.52, n.4, p.47-73
- 270 Burov, E., Gerya, T., 2014, Asymmetric three-dimensional topography over mantle plumes:
271 Nature, v.513, p.85–89
- 272 Calais, E., Freed, A., Van Arsdale, R., Stein, S., 2010, Triggering of New Madrid seismicity by
273 late-Pleistocene erosion: Nature, v.466, p.608-611
- 274 Catchings, R., 1999, Regional V_p , V_s , V_p/V_s , and Poisson's ratios across earthquake source
275 zones from Memphis, Tennessee, to St. Louis, Missouri: BSSA, v.89, p.1591-1605
- 276 Cox, R., Van Arsdale, R., 2002, The Mississippi embayment: J. Geodynamics, v.34, p.163-176
- 277 Davis, W., et al., 2021, Geochemical, petrographic, and stratigraphic analyses of the Portage
278 Lake Volcanics of the Keweenawan CFBP: Geological Society London, Special
279 Publications
- 280 Elling, R., Stein, S., Stein, C., Keller, G., 2020, Tectonic implications of the gravity signatures of
281 the Midcontinent Rift and Grenville Front: Tectonophys., v.778, pp.6
- 282 Foulger, G., 2010, Plates vs Plumes: A Geological Controversy: Wiley-Blackwell, 364 p
- 283 Gallahue, M., et al., 2020, A compilation of igneous rock volumes at volcanic passive continental
284 margins from interpreted seismic profiles: Mar. Pet. Geology, v.122, 11 p
- 285 Gordon, R., Cox, A., O'Hare, S., 1984, Paleomagnetic Euler poles and the apparent polar wander
286 and absolute motion of North America since the Carboniferous: Tectonics, v.3, p.499-537
- 287 Green, A., et al., 1989, A "GLIMPCE" of the deep crust beneath the Great Lakes, *in* Mereu, R.,
288 Mueller, S., Fountain, D., eds., Properties and Processes of Earth's Lower Crust: AGU
289 Geophys. Monograph Series 51, p.65-80
- 290 Hanson, R.E., et al., 2013, Intraplate magmatism related to the opening of the southern Iapetus
291 Ocean: Lithos., v.174, p.57-70

- 292 Hildenbrand, T., Hendricks, J., 1995, Geophysical setting of the Reelfoot Rift and relations
293 between rift structures and the New Madrid seismic zone: USGS Prof. Paper 1538-E
- 294 Hynes, A., Rivers, T., 2010, Protracted continental collision—Evidence from the Grenville orogen:
295 *Can. J. of Earth Sci.*, v.47, p.591-620
- 296 Johnson, K., 2008, Geologic history of Oklahoma. Earth sciences and mineral resources of
297 Oklahoma: Oklahoma Geological Survey Pub., v.9, p.3-5
- 298 Keller, G., Baldrige, W., 1995, The Southern Oklahoma aulacogen, *in* Olsen, K., ed., Continental
299 rifts: Evolution, structure, tectonics: Elsevier, p.427-435
- 300 Keller, G., et al., 2006, A community effort to construct a gravity database for the U.S. and an
301 associated web portal, *in* Sinha, A., ed., Geoinformatics: GSA, Boulder, CO, p.21-34
- 302 Keller, G., Lidiak, E., Hinze, W., Braile, L., 1983, The role of rifting in the tectonic development of
303 the midcontinent, U.S.A.: *Tectonophys.*, v.94, p.391-412
- 304 Keller, G., Stephenson, R., 2007, Southern Oklahoma and Dniepr-Donets aulacogens: a
305 comparative analysis, *in* Hatcher, R., Jr., et al. eds., 4-D framework of continental crust:
306 GSA Memoir 200
- 307 King, S., 2007, Hotspots and edge-driven convection: *Geology*, v.35, p.223-226
- 308 Kluth, C., Coney P., 1981, Plate tectonics of the ancestral Rocky Mountains: *Geology*, v.9, p.10-
309 15
- 310 Koptev, A., Calais, E., Burov, E., Leroy S., Gerya, T., 2015, Dual continental rift systems
311 generated by plume–lithosphere interaction: *Nature Geosci.*, v.8, p.388-392
- 312 Korenaga, J., 2013, Initiation and evolution of plate tectonics on Earth: *Ann. Rev. Earth Planet.*
313 *Sci.*, v.41, p.117-151
- 314 Lawton, T., Cashman, P., Trexler, J., Taylor, W., 2017, The late Paleozoic southwestern
315 Laurentian borderland: *Geology*, v.45, p.675-678
- 316 Leary, R., Umhoefer, P., Smith, M., Riggs, N., 2017, A three-sided orogen: A new tectonic model
317 for Ancestral Rocky Mountain uplift and basin development: *Geology*, v.45, p.735-738
- 318 Levandowski, W., Zellman, M., Briggs, R., 2017, Gravitational body forces focus North American
319 intraplate earthquakes: *Nature Comm.*, v.8, p.1-9
- 320 Li, Z.X., et al., 2008, Assembly, configuration, and break-up history of Rodinia: A synthesis:
321 *Precam. Res.*, v.160, p.179-210
- 322 Liu, L., Gao, S., Liu, K., Mickus, K., 2017, Receiver function and gravity constraints on crustal
323 structure and vertical movements of the Upper Mississippi Embayment and Ozark Uplift:
324 *J. Geophys. Res.*, v.122, p.4572-4583
- 325 Marshak, S., and van der Pluijm, B., 2021, Tectonics of the Continental Interior in the United
326 States, *in* Alderton, D., Elias, S., eds., *Encyclopedia of Geology*: Academic Press, v.4,
327 p.173-186

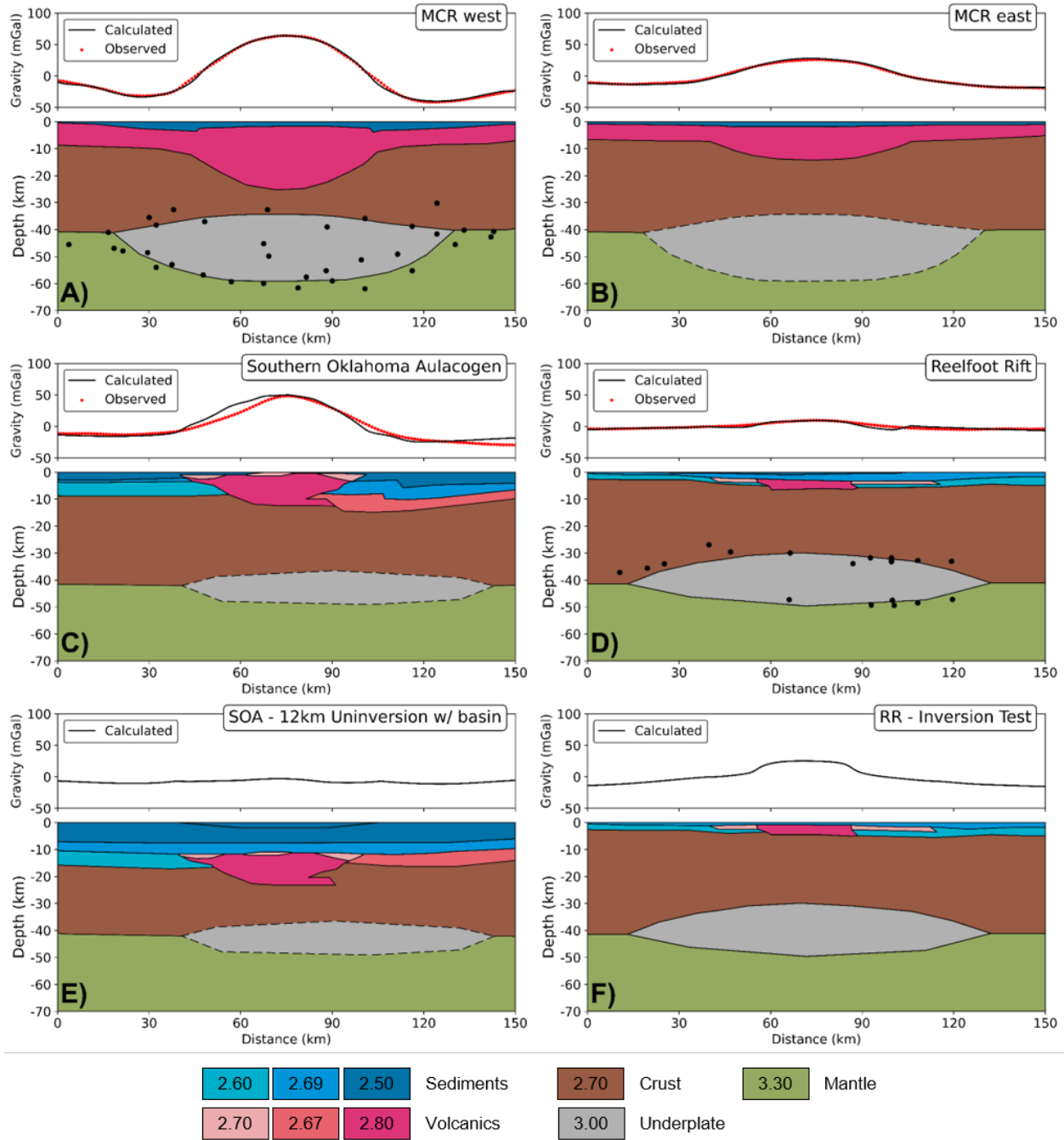
- 328 Mayhew, M., Thomas, H., Wasilewski, P., 1982, Satellite and surface geophysical expression of
329 anomalous crustal structure in Kentucky and Tennessee: *Earth Planet. Sci. Lett.*, v.58,
330 p.395-405
- 331 Merino, M., Keller, G., Stein, S., Stein, C., 2013, Variations in Mid-Continent Rift magma volumes
332 consistent with microplate evolution: *Geophys. Res. Lett.*, v.40, p.1513-1516
- 333 Mooney, W., et al., 1983, Crustal structure of the Northern Mississippi Embayment and a
334 comparison with other continental rift zones: *Tectonophys.*, v.94, p.327-348
- 335 Nelson, K., Zhang, J., 1991, A COCORP deep reflection profile across the buried Reelfoot rift:
336 *Tectonophys.*, v.197, p.271-293
- 337 Nicholson, S., Shirey, S., Schulz, K., and Green, J., 1997, Rift-wide correlation of 1.1 Ga
338 Midcontinent rift system basalts: *Can. J. Earth Sci.*, v.34, p.504-520
- 339 Ojakangas, R., Morey, G., Green, J., 2001, The Mesoproterozoic midcontinent rift system: *Sed.*
340 *Geol.*, v.141, p.421-442
- 341 Perry, W., Jr., 1989, Tectonic evolution of the Anadarko basin region: *USGS Bull.* 1866
- 342 Richards, M., Duncan, R., Courtillot, V., 1989, Flood basalts and hot-spot tracks: *Science*, v.246,
343 p.103-107
- 344 Rooney, T., et al., 2017, The making of an underplate: pyroxenites from the Ethiopian lithosphere:
345 *Chem. Geol.*, v.455, p.264-281
- 346 Sandwell, D., et al., 2013, Towards 1 mGal global marine gravity from CryoSat-2, Envisat, and
347 Jason-1: *Leading Edge*, v.32, p.892-899
- 348 Scotese, C., Elling, R., 2017, Plate tectonic evolution during the Last 1.3 billion Years: William
349 Smith Meeting 2017: Plate Tectonics at 50. *Geol. Soc. London*
- 350 Shay, J., Trehu, A., 1993, Crustal structure of the central graben of the Midcontinent Rift beneath
351 Lake Superior: *Tectonophys.*, v.225, p.301-335
- 352 Stein, C., et al., 2014, Was the Mid-continent Rift part of a successful seafloor spreading
353 episode?: *Geophys. Res. Lett.*, v.41, p.1465-1470
- 354 Stein, C., Kley, J., Stein, S., Hindle, D., Keller, G., 2015, North America's Midcontinent Rift: when
355 rift met LIP: *Geosphere*, v.11, p.1607-1616
- 356 Stein, C., Stein, S., Elling, R., Keller, G., Kley, J., 2018, Is the "Grenville Front" in the central
357 United States really the Midcontinent Rift?: *GSA Today*, v.28, p.4-10
- 358 Stein, C., Stein, S., Gallahue, M., Elling, R., 2021, Revisiting hotspots and continental breakup –
359 Updating the classic three-arm model, In the Footsteps of Warren Hamilton: Special
360 Paper, GSA, in press
- 361 Stein, S., et al., 2018, Insights from North America's failed Midcontinent Rift into the evolution of
362 continental rifts and passive continental margins: *Tectonophys.*, v.744, p.403-421

- 363 Swanson-Hysell, N., Ramezani, J., Fairchild, L., Rose, I., 2019, Failed rifting and fast drifting:
364 Midcontinent Rift development, Laurentia's rapid motion and the driver of Grenvillian
365 orogenesis: *GSA Bull.*, v.131, p.913-940
- 366 Thomas, W., 2011, The Iapetan rifted margin of southern Laurentia: *Geosphere*, v.7, p.97-120
- 367 Thybo, H., Artemieva, I., 2013, Moho and magmatic underplating in continental lithosphere:
368 *Tectonophys.*, v.609, p.605–619
- 369 Tohver, E., D'Agrella-Filho, M., Trindade, R., 2006, Paleomagnetic record of Africa and South
370 America for the 1200-500 Ma interval, and evaluation of Rodinia and Gondwana
371 assemblies: *Precam. Res.*, v.147, p.193-222
- 372 van Wijk, J., Huismans, R., Ter Voorde, M., Cloetingh, 2001, Melt generation at volcanic
373 continental margins: no need for a mantle plume: *Geophys. Res. Lett.*, v.28, p.3995-3998
- 374 Vervoort, J., Wirth, K., Kennedy, B., Sandland, T., Harpp, K., 2007, Magmatic evolution of the
375 Midcontinent rift: *Precam. Res.*, v.157, p.235-268
- 376 Wall, C., et al., 2020, Integrating zircon trace-element geochemistry and high-precision U-Pb
377 zircon geochronology to resolve the timing and petrogenesis of the late Ediacaran-
378 Cambrian Wichita igneous province, Southern Oklahoma Aulacogen: *Geology*, v.49,
379 p.268-272
- 380 Walper, J., 1977, Paleozoic tectonics of the southern margin of North America: Gulf Coast
381 Association of Geological Societies Transactions, v.27, p.230-241
- 382 White, R., 1997, Mantle temperature and lithospheric thinning beneath the Midcontinent rift
383 system: *Can. J. Earth Sci.*, v.34, p.464-475
- 384 White, R., McKenzie, D., 1989, Magmatism at rift zones: *J. Geophys. Res.*, v.94, p.7685-7729
- 385 Whitmeyer, S., and Karlstrom, K., 2007, Tectonic model for the Proterozoic growth of North
386 America: *Geosphere*, v.3, p.220-259
- 387 Zhang, H., et al., 2016, Distinct crustal structure of the North American Midcontinent Rift from P
388 wave receiver functions: *J. Geophys. Res.*, v.121, p.8136-8153



389

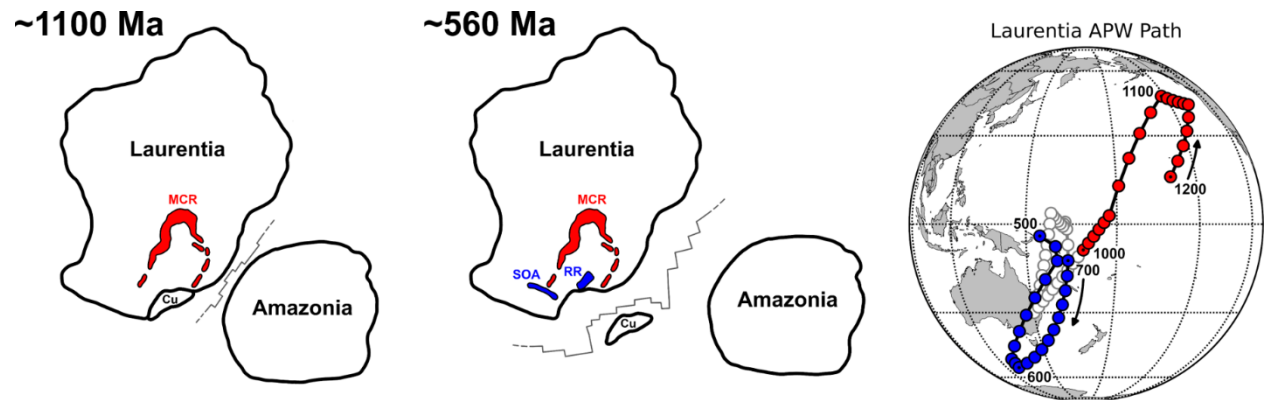
390 Fig. 1: (A) Bouguer gravity anomaly map for central North America. Anomalies related to the
 391 Midcontinent Rift, Southern Oklahoma Aulacogen, and Reelfoot Rift are outlined. Dashed lines
 392 outline possible extensions of rift arms not included in analysis. (B) Profiles used in calculating
 393 the average gravity anomalies. (C) Mean anomalies and standard deviations for rifts.



394

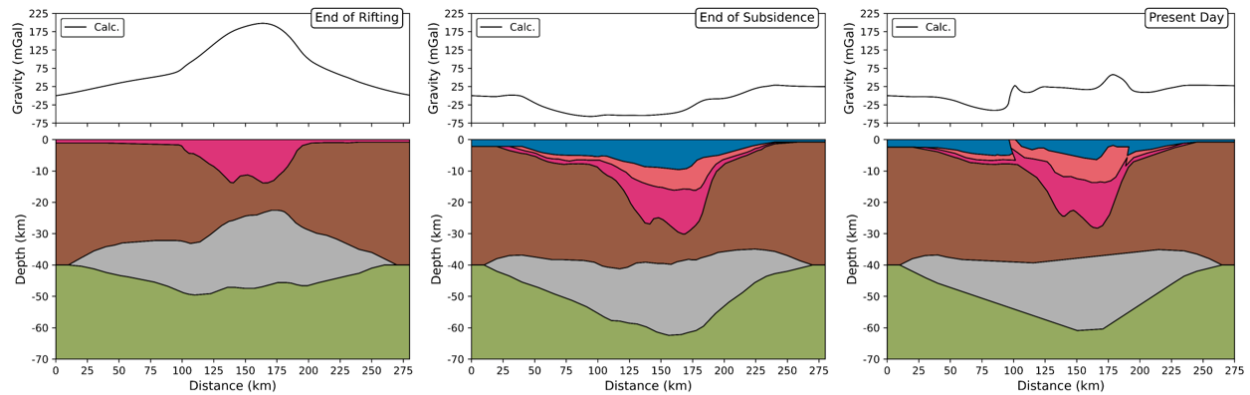
395 Fig. 2: Gravity data and rift models. (A) West MCR arm, with underplate based on receiver function
 396 data (dots). (B) East MCR arm, modeled with underplate like the west arm's, dashed given its
 397 uncertainty. (C) Southern Oklahoma Aulacogen, with proposed underplate dashed given its
 398 uncertainty. (D) Reelfoot Rift, with underplate based on receiver function data (dots). (E) Model
 399 for the SOA if it had not been inverted, leaving a smaller positive anomaly. (F) Model for the RR
 400 if it had been inverted, producing a positive anomaly. Densities in g/cm^3 .

401



402

403 Fig. 3: (Left) Schematic reconstruction of plate positions relative to Laurentia ~1100 Ma during
 404 formation of Rodinia. Between collisional phases of the Grenville orogeny, a spreading likely
 405 opened between the major plates. Following failure of the MCR, Amazonia shifted north along the
 406 margin before recolliding. (Center) Similar reconstruction at ~560 Ma as Rodinia was breaking
 407 up. Cuyania (Cu) block rifted off Laurentia, leaving SOA and RR as failed arms. (Right) Apparent
 408 polar wander path of Laurentia, plotted in present-day coordinates, at 10-myr increments. Red
 409 cusp (1200-1000 Ma) is related to formation of the MCR, and blue cusp (700-500 Ma) is related
 410 to initial rifting of the SOA and RR. Path between these events plotted in grey.



411
 412 Fig. 4: Gravity anomalies expected at various stages in rift evolution, based on model for MCR
 413 under Lake Superior. In early stages, dense volcanics cause a large positive anomaly.
 414 Subsequent deposition of low-density sediments and associated subsidence cause a gravity low.
 415 Inversion of the rift and erosion of low-density sediments cause the high observed today.
 416 Densities in g/cm³. (After Elling et al., 2020).